Published by
NIGERIAN SOCIETY OF PHYSICAL SCIENCES
Available online @ https://journal.nsps.org.ng/index.php/jnsps

J. Nig. Soc. Phys. Sci. 8 (2026) 3259

Check for updates

Journal of the Nigerian Society of Physical Sciences

Numerical study of hall current and thermophoresis effect on the hydromagnetic casson nano fluid flow over a stretching surface

Jatin Kumar[a], Khem Chand[a], Pankaj Thakur[b,*]

[a]Department of Mathematics & Statistics, Himachal Pradesh University Summer Hill, Shimla-171005, India
[b]Department of mathematics, ICFAI University, Himachal Pradesh, Solan, India

Abstract

This study investigate, the numerical analysis of heat and mass transfer in Hydro magnetic Casson Nano particle flow past a stretching surface by including the effect of Hall current, thermophoresis and inclined magnetic field. The governing partial differential equations are transformed into nonlinear ordinary differential equations through similarity transformations and then solved by using the MATLAB inbuilt bvp4c method.The variations due to the key parameters occurring in the governing mathematical formulations on temperature, rate of flow and concentration profile are presented graphically and the variations in the primary attributes of the flow field namely, skin friction,Sherwood and Nusselt number are presented through a table. The outcomes of the analysis show that the Hall current parameter (m) increases the transverse velocity while it decreases the temperature and nanoparticle concentration. On the other hand increasing magnetic field parameter (M) enhance the nanoparticle concentration and it decreases the tangential and transverse velocities. The thermophoresis parameter (Nt) results in increasing the temperature and concentration profile. The inclination angle (γ) with the vertical axis reduces the velocity profiles. The analysis provides a valuable insight in optimizing the transport of heat and mass in hydro magnetic Casson Nano fluid flow systems which will find applications in advanced cooling and thermal management technologies.

DOI:10.46481/jnsps.2026.3259

Keywords: Hall current, Casson fluid, Stretching surface, bvp4c.

Article History:
Received: 05 January 2026
Received in revised form: 03 March 2026
Accepted for publication: 17 April 2026
Available online: 14 May 2026

Communicated by: ******

1. Introduction

Due to the non- linear and complex dependence of shear stress on shear strain rate in non newtonian fluids, there is a lot of interest in the real world uses for non-newtonian fluid theory. When small amount of shear stress is applied to these fluids, they usually show the characteristics of elastic solids, which stops them from flowing. A different type of non-Newtonian liquid is the Casson fluid system. This system was first introduced by Casson in 1959 [1].

It is based on the structural properties of the fluid state and its interacting behaviour of solids in a dual-phase system. Casson fluids include things like tomato sauce, honey, jelly and concentrated fruit juices. Since the existence of proteins, globulin, fibrinogen and red blood cells floating in plasma in human blood. The most frequently utilized non-newtonian fluid is Casson fluid which has a significant use in different areas such as mechanical, chemical and bio-engineering. The modeling and numerical simulation of hydro-magnetic organic Convection of Casson fluid flow which involve a chemical interaction of higher order and heating in porous media have been recently discussed by Seth and Bhattacharyya [2].

In the presence of heat energy, Pramanik [3] resolved the

*Corresponding author Tel. No: +918570975865
Email address: pankaj@journal.nsps.org.ng (Pankaj Thakur)

Casson flow problem through an exponentially porous stretching surface. MHD stretching of Casson Nano fluid movement between convectively heated disks in parallel was studied by Umavathi *et al.* [4]. Thermal analysis and the creation of entropy for the rotational motion of a hydro magnetic Casson Nano fluid past a revolving cylinder with Joule effect was investigated by Arshad Khan *et al.* [5]. Unstable MHD oscillatory Casson flow through tilted vertical porous plate applying Soret effects and radiation absorption has been explored by Raghunath and Obulesu [6] . Recently, the Casson Nano fluid flow through an stretched surface was quantitatively investigated by Senapati *et al.* [7].

Certain molecules carrying electrical charge can divert from their normal path due to a high magnetic field arising from the Hall effect or Lorentz force. The magnitude and direction density of electrical current indicate in evident that Hall current has a major effect on the magnetic force. Convective flow problems with magnetic fields caused by Hall current are important for engineering applications in MHD engines, power plants, refrigeration tubes, electric transformers and transmission paths, nanotechnology processing,nuclear power plants that use molten metals, heating units and regulating of blood flow. When the magnetic intensity is large and specific mass of gas is small, than analysis of MHD flow by hall component of electric current has the highly uses in the analysis of flight MHD and the hall acceleration devices.

Under the impact of outer magnetic fields, peristalsis flow has multiple uses in the oxygenation, hypothermia, process of dialysis and MHD functions of blood. There are many applications in the area of food engineering, power engineering, petroleum production and plastics processing industry. Eldahab [8] used a stretched sheet for investigating the hall effects and free convective MHD flow. Thamizsudar [9] studied how rotation and Hall current affected the mass and heat movement of an MHD fluid flow across a vertical plate with exponential acceleration. Laxmi *et al.*[10] analysis the steady 2D hybrid casson nanoparticle through a extensional surface using magnetohydrodynamic effects and porous medium. Sharma *et al.* [11] studied the thermal instability of rotating Jeffrey nanofluids in porous media with variable gravity, highlighting its effects on heat transfer and flow behavior.

Buongiorno [12] used a mathematical system that incorporates two key mechanisms thermos-diffusion and Brownian motion to study the convective heat transport of Nano liquids. The behaviour of the outer layer of the Nanoparticle towards an upright Flat plates have been investigated by Kuznetsov and Nield [13] by applying the model given by Buongiorno. Sharma *et al.* [17] investigated electrohydrodynamic convection in a dielectric rotating Oldroydian nanofluid within a porous medium, emphasizing its impact on flow and heat transfer characteristics.

Khan and Pop[14] look into the emission of the boundary layer of nanomaterials across a plate which is horizontal. They treated the nonlinear problem using the Keller box approach and discovered that the concentration of the layer structure within the nanoparticles is reduced by the mechanism associated with their Brownian movement. Sharma *et al.*[18] analysis the influnce of flow on bidisperse convection in Rivilin Ericksen viscoelastic fluid which saturated in a permeable formation. The current study is an extension of Wahid Owhaib *et al.* [15]. Here we study, the core objective is to investigate of the mass and heat transfer in three dimensional Hydro magnetic Casson Nano particle movement across a stretching surface in the presence of hall current, brownian motion and thermophoresis.

Pr	Gorla and sidawi [16]	Present
2	0.9114	0.9465
3	1.1597	1.2296
7	1.8904	1.9249
10	2.3035	2.3248
50	5.4247	5.3220
70	6.4622	6.4513

Table 1. Evaluation of $-\theta'(0)$ for various Prandtl numbers.

The nonlinear partial differential equations which describing mass, heat and flow transfer are reformulated to ODEs by similarity transformations which are eventually resolved numerically. Buongiorno system is used to include the thermosmigration and irregular movement of the nanoparticle. The system of eqs solved by MATLAB bvp4c coding. The outcomes are discussed and presented in graphs to show the behaviour of several non-dimensional governing variables like as brownian motion (Nb), lewis number(Le), thermophoresis parameter(Nt), casson fluid(Ca), Prandtl number (Pr), magnetic number(M), hall induced current (m) and Inclined angle (γ) on temperature, flow rate and concentration profiles.

The results of this study are correlate well with the outcomes from previous studies under comparable conditions. The present study focuses on Casson nanofluid behavior under hall current and thermophoretic effects, but we firmly believe that hybrid nanofluids and multicomponent suspensions always represent a promising direction for further work as it can find feasible experimental applications in setups such as MHD flow loop systems with controllable inclined magnetic field and electrically conducting Casson-type fluids (i.e., polymer-based suspension etc).

2. Mathematical formulation

In this model we consider the laminar steady flow regime, three dimensional motion of an electrically conductive incompressible casson nano fluid over a stretching surface is considered.The Cartesian coordinate system is chosen such that the stretching plate lies in the xy-plane and the fluid occupies the domain where $z \geq 0$, with the positive z-direction across the plate. A constant magnetic field having strength B_0 is applied, making an angle γ with the positive z-axis. The temperature of liquid away from the stretching surface is denoted by T_∞ and the surface is assumed to move in the xy-plane. Figure 1 shows the physical configuration considered.

Using Prandtl's boundary layer method in the problem under study the governing equation by following [12], [16] can be taken as under.

Table 2. The numerical outputs for skin friction, sherwood number and nusselt number under different parameter are given.

M	m	Ca	Nb	Nt	Pr	Le	$-C_f$	Nu	Sh
0.1	0.1	0.2	0.5	0.5	0.2	1.0	0.632380416	-0.000452239	0.528345781
0.5							0.601873604	-0.002385953	0.528270031
1.0							0.562107036	-0.005128971	0.528525571
0.1	0.5						0.601873604	-0.002385953	0.528270031
	1.0						0.562107036	-0.005128971	0.528525571
	1.5						0.520372902	-0.008318640	0.529226240
	0.1	0.3					0.769025443	-0.000582122	0.531745959
		0.4					0.885664831	-0.000689290	0.537583265
		0.5					0.989017989	-0.000781883	0.544372361
		0.2	0.6				0.632380415	-0.000452239	0.561821958
			0.7				0.632380417	-0.000452239	0.586011109
			0.8				0.632380417	-0.000452239	0.604406247
		0.5	0.6				0.632380417	-0.000452239	0.555710058
			0.7				0.632380417	-0.000452239	0.616438200
			0.8				0.632380419	-0.000452239	0.727226412
		0.5	1.0				0.632380458	-0.000452238	0.429888532
			2.0				0.632380458	-0.000452238	0.366440121
			0.8				0.632380458	-0.000452238	0.332214868
		0.2		1.5			0.632380418	-0.000452239	0.726072196
				2.0			0.632380419	-0.000452239	0.893935989
				2.5			0.632380420	-0.000452239	1.040818594

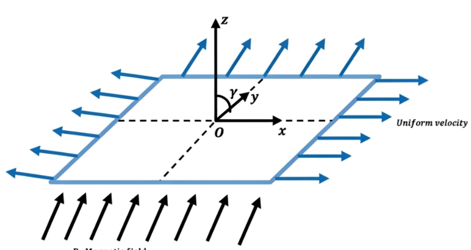

Figure 1. Configuration of the system.

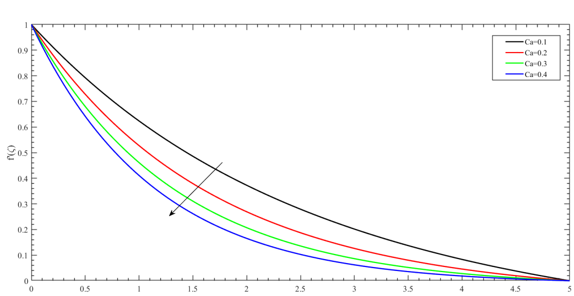

Figure 2. Effectiveness of the the Casson parameter Ca on $f'(\zeta)$.

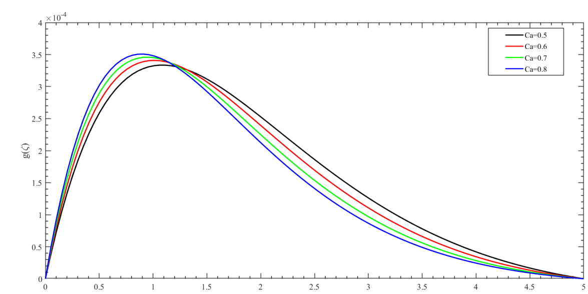

Figure 3. Effectiveness of the Casson parameter Ca on $g(\zeta)$.

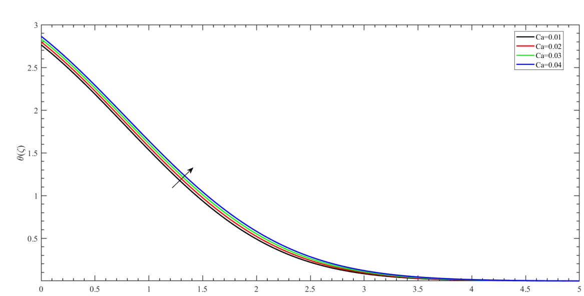

Figure 4. Effectiveness of the Casson non-Newtonian factor Ca on $\theta(\zeta)$

Using Prandtl's boundary layer method in the problem under study the governing equation by following [12], [16] can be taken as under.

$$\frac{\partial u}{\partial x}+\frac{\partial v}{\partial y}+\frac{\partial w}{\partial z}=0 \quad (1)$$

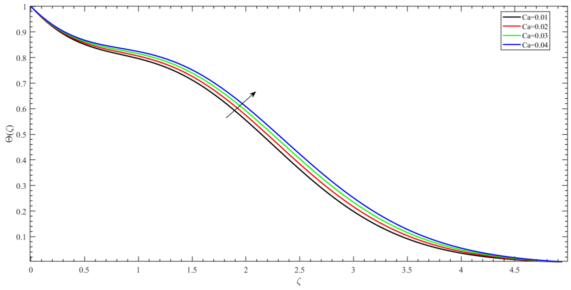

Figure 5. Effectiveness of the Casson factor Ca on concentration, $\Phi(\zeta)$.

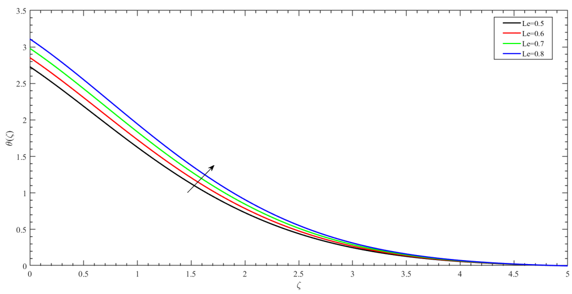

Figure 6. Effectiveness of Le, on temperature, $\theta(\zeta)$.

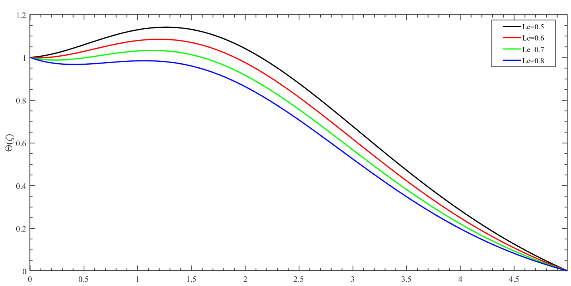

Figure 7. Effectiveness Le, on concentration, $\phi(\zeta)$.

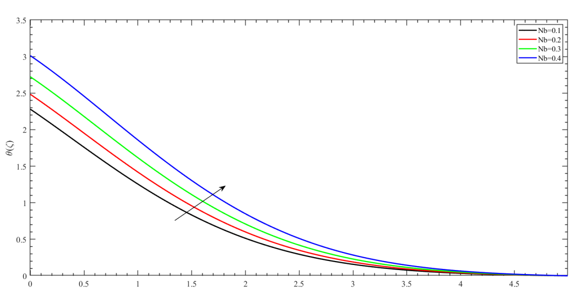

Figure 8. Effectiveness of Nb, on temperature, $\theta(\zeta)$.

$$\frac{\partial u}{\partial x} + \frac{\partial v}{\partial y} + \frac{\partial w}{\partial z} = 0 \tag{2}$$

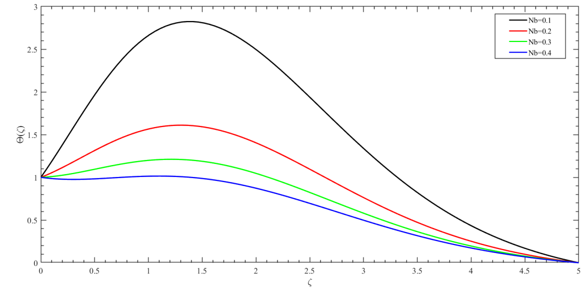

Figure 9. Effectiveness of Nb on concentration, $\phi(\zeta)$.

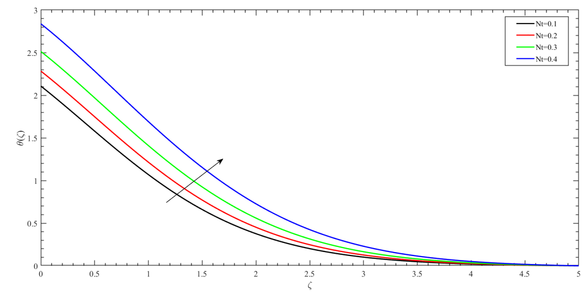

Figure 10. Effectiveness of Nt on temperature, $\theta(\zeta)$.

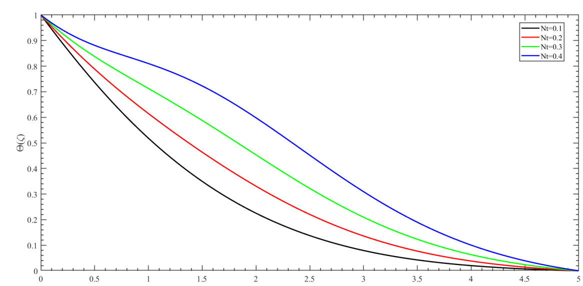

Figure 11. Effectiveness of Nt on concentration, $\phi(\zeta)$.

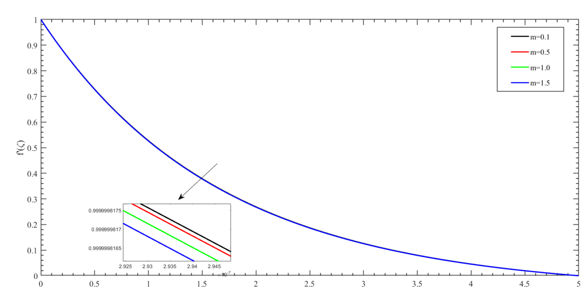

Figure 12. Effectiveness of Hall current, m on $f'(\zeta)$.

2.1. Numerical method

Matlab bvp4c method is employed to obtain the numerical solution of the non-linear boundary value problem. This is done by letting

$$f = y_1, \quad f' = y_2, \quad f'' = y_3, \quad g = y_4, \quad g' = y_5, \quad \theta = y_6,$$

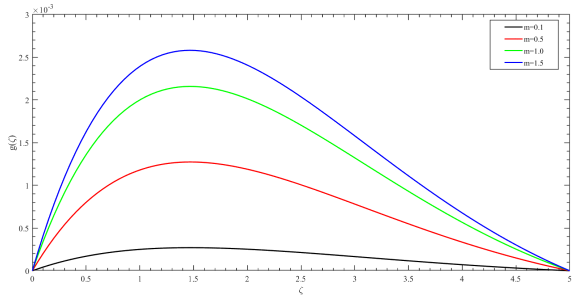

Figure 13. Effectiveness of Hall current, m on $g(\zeta)$.

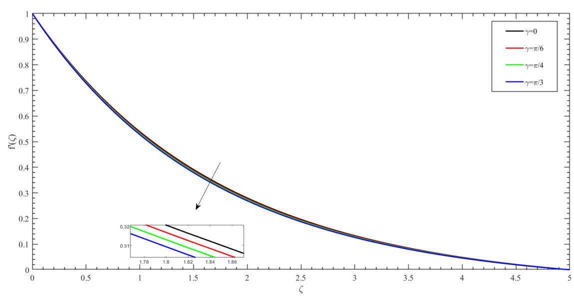

Figure 14. Effectiveness of transverse velocity, $f'(\zeta)$ with angle γ.

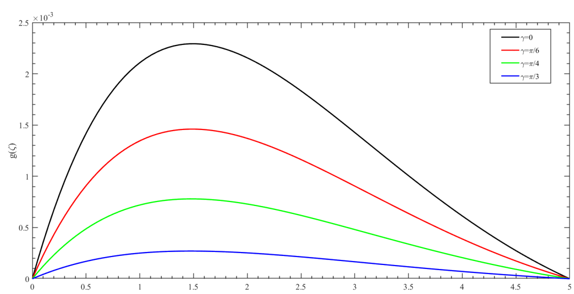

Figure 15. Effectiveness of transverse velocity, $g(\zeta)$ with angle γ.

$$\theta' = y_7, \quad \Theta = y_8, \quad \Theta' = y_9,$$

which results in the first-order differential equation system that follows:

$$y_1' = y_2$$

$$y_2' = y_3$$

$$y_3' = \frac{Ca}{1+Ca}\left(y_2^2 - y_1 y_3 + \frac{M\,(m y_4 \cos\gamma - y_2)\cos^2\gamma}{1+m^2\cos^2\gamma}\right)$$

$$y_4' = y_5$$

$$y_5' = \frac{Ca}{1+Ca}\,y_2 y_4 \;-\; y_1 y_5 \;+\; \frac{M\,(m y_2 \cos\gamma + y_4)\cos^2\gamma}{1+m^2\cos^2\gamma}$$

$$y_6' = y_7$$

$$y_7' = -\Pr\left(y_1 y_7 + Nb\,y_7 y_9 + Nt\,y_7^2\right)$$

$$y_8' = y_9$$

$$y_9' = -Le\,y_1 y_9 \;+\; \frac{Nt}{Nb}\,\Pr\left(y_1 y_7 + Nb\,y_7 y_9 + Nt\,y_7^2\right),$$

with,

$$y_1(0) = y_4(0) = 0, \quad y_2(0) = y_8(0) = 1, \quad y_7(0) = -1,$$

$$y_2(\infty) = y_4(\infty) = y_6(\infty) = y_8(\infty) = 0.$$

The resulting first-order system of governing equations is numerically solved by MATLAB's `bvp4c` routine which is designed for boundary value problems expressed as

$$y' = f(x, y),$$

along with appropriate boundary conditions. The routine employs the FDM, achieving an prediction accuracy of up to 10^{-9}. To ensure accuracy, the numerical solution obtained for $-\theta'(0)$ is measured with results from previous studies under the conditions $Nt = \gamma = M = m = \phi = Le = Ca = 0$, while Nb varies from 0.1 to 2.3. The results of this study are similar to those mentioned in the literature, as Table 1 shows below. In this subsequent, a parametric invistegated is conducted.

2.2. Discussion of findings

To present the effectiveness of relevant parameters on the temperature, flow rate and concentration profile of Casson nanofluid, the expressions obtained above are interpreted with the help of graphs presented in Figures 2–15 and discussed in detail. Figures 2–5 illustrate the manner in which the Casson fluid parameter Ca alters the temperature $\theta(\zeta)$, nanoparticle concentration $\phi(\zeta)$ and flow rate $f'(\zeta)$ and $g(\zeta)$. As the computed value of Ca increases, a downfall behaviour is observed for the axial flow speed layer $f'(\zeta)$, as shown in Figure 2, while the temperature and nano fluid concentration profiles exhibit the reverse trend, as seen in Figures 4 and 5. The transverse velocity $g(\zeta)$, illustrated in Figure 3, first increases in magnitude near the boundary and then decreases distant from the surface.

The Figures 6 & 7 show that higher in Lewis number Le, correlates to a less mass diffusivity and higher thermal diffusivity. Stronger thermal diffusivity produces a thin thermal layer structure, as seen in Figure 6. A reduced mass diffusivity, as observed in Figure 7, generates a thinner concentration layer structure of nanoparticles.

The Figures 8–11 are used for studying how nanoparticles affect the Casson fluid dynamics through thermos-diffusion of nanoparticles (Nt) and Brownian movement(Nb). The enhancement to the thermal field occurs by the random movement of nanoparticles, which collide and produce additional internal heat within the Casson fluid as show in Figure 8. As the Nb values increased, the concentration field of nanoparticles is decreased as show in Figure 9. However, the mechanism of thermophoresis is associated with a thermal gradient, which generates extra heat in the system of Casson fluid, increasing the temperature and concentration gradients of nanoparticles as in show Figures 10 & 11. nanoparticles as in show Figure 10 & 11.

Therefore, the results suggest that the temperature of Casson particle significantly enhanced by transmitting nanoparticle.

Figures 12 and 13 show the influence of the hall conductivity factor, m on axial velocity, $f'(\zeta)$ and transverse velocity, $g(\zeta)$ profiles respectively. It is clear to Figures12 and 13 that increasing the Hall effect factor m causes the transverse rate of flow $g(\zeta)$ to increase, while the tangential rate of flow $f'(\zeta)$ decreases.

Figures 14 & 15 show the influence of inclined angle on flow rate factor. It is found that when the flow rate decrease as tilted angle, γ is higher.

In accordance of Table 2, the analysis reveals that the skin friction in the x-direction increases with enhancement in the hall conductivity factor m along with the strengthness in magnetic field parameter M, whereas it slow down with rising values of the Brownian motion parameter Nb, casson fluid parameter Ca, and thermophoresis factor Nt. The Nusselt number remains unchanged when the Brownian motion parameter Nb, Prandtl number Pr, thermophoresis parameter Nt and Lewis number Le increase, whereas it decreases with higher values of the the magnetic influence parameter M, the Hall effect factor m, and the Casson model parameter Ca. Furthermore, the Table illustrates that the Sherwood number decreases with the Prandtl number (Pr), while it increases with the magnetic parameter (M), Hall current parameter (m), Casson fluid parameter (Ca), Brownian motion parameter (Nb), Lewis number (Le) and thermophoresis parameter (Nt). Numerical values of skin friction $\left(\mathrm{Re}_x^{1/2} C_{fx}\right)$, Nusselt number $\left(\mathrm{Re}_x^{1/2} Nu_x\right)$ and Sherwood number $\left(\mathrm{Re}_x^{1/2} Sh_x\right)$ can be found in Table 2.

3. Conclusion

The current investigation presents a comprehensive analysis of the thermal and mass transfer behaviour of Hydromagnetic Casson Nano particle flow through a starching surface, considering various influencing factors involving in the governing equations. It can find feasible experimental applications in setups such as MHD flow loop systems with controllable inclined magnetic field and electrically conducting Casson-type fluids. The major conclusion obtained from the study:

- The concentration of nanofluid and the transverse as well as the axial velocities rises with an increase in the magnetic field factor. This indicates that an increased in magnetic field give more effective concentration of nanoparticles in the fluid.
- The Hall parameter has a dual effect, it increases the transverse velocity and temperature but decreases in nanoparticle concentration. This means that Hall effect can significantly change the flow motion and the thermal behaviour of the nanofluid.
- The Casson fluid factor is found to reduce tangential velocity but increase temperature and nanoparticle concentration. This highlights the importance of the fluid's rheological properties in influencing flow behavior and thermal performance.
- Higher Lewis numbers correspond to thicker thermal layers and thinner concentration layers. This relationship suggests that thermal diffusivity has significant effects on the development of thermal and mass-diffusion characteristics during the heat transfer process.

3.1. Nomenclature

Symbol	Description
r, x	Cylindrical polar coordinates
a	Stretching parameter
u	Velocity component along x-axis
v	Velocity component along y-axis
w	Velocity component along z-axis
u_w	Surface velocity
v_w	Wall mass transfer velocity
ψ	Stream function
Le	Lewis number
B_0	Applied magnetic field
T	Fluid temperature
T_∞	Free stream temperature
ξ	Similarity variable
γ	Angle of magnetic field
ϕ_{s1}	Volume fraction of alumina nanoparticles
ϕ_{s2}	Volume fraction of copper nanoparticles
m	Hall current parameter
f	Dimensionless axial velocity
g	Dimensionless transverse velocity
θ	Dimensionless temperature
S	Mass transfer parameter
K	Darcy permeability
k_f	Thermal conductivity of fluid
k_{hnf}	Thermal conductivity of hybrid nanofluid
ρ_{hnf}	Density of hybrid nanofluid
$(\rho C_p)_f$	Heat capacity of fluid
$(\rho C_p)_{hnf}$	Heat capacity of hybrid nanofluid
μ_f	Dynamic viscosity of fluid
μ_{hnf}	Dynamic viscosity of hybrid nanofluid
σ_f	Electrical conductivity of fluid
σ_{hnf}	Electrical conductivity of hybrid nanofluid
β_f	Thermal expansion coefficient of fluid
β_{hnf}	Thermal expansion coefficient of hybrid nanofluid
β_{s1}	Thermal expansion coefficient of alumina
β_{s2}	Thermal expansion coefficient of copper
Ca	Casson fluid parameter
Pr	Prandtl number
Nb	Brownian motion
Nt	Thermophoretic coefficient
Φ	Nanofluid concentration
ρ	Specific mass of fluid
μ	Internal friction of fluid
C_p	Heat capacity

Symbol	Description
k	Thermal transfer coefficient
D_B	Brownian diffusion coefficient
D_T	Thermophoretic diffusion coefficient
α	Thermal diffusion coefficient
C_f	Local skin friction coefficient
q_w	Thermal energy flux
C	Concentration
ν	Momentum diffusivity
S_f	Friction factor
S_h	Sherwood number
Nu_x	Local Nusselt number
Re_x	Local Reynolds number

4. Data availability

In this study, no primary datasets were generated or collected.

References

[1] N. Casson, "A flow equation for pigment-oil suspensions of the printing ink type", (1959) 84–104. https://ci.nii.ac.jp/naid/10019819064.

[2] G. S. Seth, A. Bhattacharyya, R. Kumar & M. K. Mishra, "Modeling and numerical simulation of hydromagnetic natural convection Casson fluid flow with nth-order chemical reaction and Newtonian heating in porous medium", Journal of Porous Media **22** (9) (2019) 1141–1157. https://doi.org/10.1615/JPorMedia.2019025699.

[3] S. Pramanik, "Casson fluid flow and heat transfer past an exponentially porous stretching surface in presence of thermal radiation", Ain Shams Engineering Journal **5** (1) (2014) 205–212. https://doi.org/10.1016/j.asej.2013.05.003.

[4] J. C. Umavathi, "Magnetohydrodynamic squeezing Casson nanofluid flow between parallel convectively heated disks", International Journal of Modern Physics B **37** (4) (2023) 2350031. https://doi.org/10.1142/S0217979223500315.

[5] A. Khan, Z. Shah, E. Alzahrani & S. Islam, "Entropy generation and thermal analysis for rotary motion of hydromagnetic Casson nanofluid past a rotating cylinder with Joule heating effect", International Communications in Heat and Mass Transfer **119** (2020) 104979. https://doi.org/10.1016/j.icheatmasstransfer.2020.104979.

[6] K. Raghunath & M. Obulesu, "Unsteady MHD oscillatory Casson fluid flow past an inclined vertical porous plate in the presence of chemical reaction with heat absorption and Soret effects", Heat Transfer **51** (3) (2021) 1–19. https://doi.org/10.1002/htj.22327.

[7] M. Senapati, K. Swain & S. K. Parida, "Numerical analysis of three-dimensional MHD flow of Casson nanofluid past an exponentially stretching sheet", Karbala International Journal of Modern Science **6** (1) (2020) 13. https://doi.org/10.33640/2405-609X.1462.

[8] E. M. Abo-Eldahab, "Hall effects on magnetohydrodynamic free-convection flow at a stretching surface with a uniform free stream", Physica Scripta **63** (2001) 29–35. http://dx.doi.org/10.1238/Physica.Regular.063a00029.

[9] M. Thamizhsudar, J. Pandurangan & R. Muthucumaraswamy, "Hall effects and rotation effects on MHD flow past an exponentially accelerated vertical plate with combined heat and mass transfer effects", International Journal of Applied Mechanics and Engineering **20** (3) (2015) 605–616. https://doi.org/10.1515/ijame-2015-0039.

[10] B. Laxmi, K. Chand & P. Thakur, "Hydrodynamic Casson hybrid nanofluid flow across a stretching sheet in the regime of velocity slip and temperature jump, including viscous dissipation, melting, Soret and Dufour effects", Journal of the Nigerian Society of Physical Sciences **7** (4) (2025) 2936. https://doi.org/10.46481/jnsps.2025.2936.

[11] P. L. Sharma, D. Bain & P. Thakur, "Thermal instability of rotating Jeffrey nanofluids in porous media with variable gravity", Journal of the Nigerian Society of Physical Sciences **5** (2) (2023) 1366. https://doi.org/10.46481/jnsps.2023.1366.

[12] J. Buongiorno, "Convective transport in nanofluids", ASME Journal of Heat Transfer **128** (3) (2006) 240–250. https://doi.org/10.1115/1.2150834.

[13] A. V. Kuznetsov & D. A. Nield, "Natural convective boundary-layer flow of a nanofluid past a vertical plate", International Journal of Thermal Sciences **49** (2) (2010) 243–247. https://doi.org/10.1016/j.ijthermalsci.2009.07.015.

[14] W. A. Khan & I. Pop, "Boundary-layer flow of a nanofluid past a stretching sheet", International Journal of Heat and Mass Transfer **53** (11) (2010) 2477–2483. https://doi.org/10.1016/j.ijheatmasstransfer.2010.01.032.

[15] W. Al-Kouz & W. Owhaib, "Numerical analysis of Casson nanofluid three-dimensional flow over a rotating frame exposed to a prescribed heat flux with viscous heating", Scientific Reports **12** (2022) 4256. https://doi.org/10.1038/s41598-022-08211-2.

[16] R. S. R. Gorla & I. Sidawi, "Free convection on a vertical stretching surface with suction and blowing", Applied Scientific Research **52** (1994) 247–257. https://doi.org/10.1007/BF00853952.

[17] P. L. Sharma, "Electrohydrodynamics convection in dielectric rotating Oldroydian nanofluid in porous medium", Journal of the Nigerian Society of Physical Sciences **5** (2) (2023) 1231. https://doi.org/10.46481/jnsps.2023.1231.

[18] P. L. Sharma, D. Bains & P. Thakur, "Throughflow effect on bi-disperse convection in Rivlin–Ericksen fluid", Journal of the Nigerian Society of Physical Sciences **6** (3) (2024) 2052. https://doi.org/10.46481/jnsps.2024.2052.